

## Electronic Supplementary Information (ESI)

### Polymorphic transformations and optical properties of graphene based Ag doped titania nanostructures

*Mohan Chandra Mathpal<sup>1,2</sup>, Anand Kumar Tripathi<sup>1</sup>, Promod Kumar<sup>3</sup>, Balasubramaniyan. R<sup>2</sup>,  
Manish Kumar Singh<sup>4</sup>, Jin Suk Chung<sup>\*2</sup>, Seung Hyun Hur<sup>2</sup>, Arvind Agarwal<sup>1</sup>*

*<sup>1</sup>Department of Physics, Motilal Nehru National Institute of Technology, Allahabad-211004,  
India*

*<sup>2</sup>School of Chemical Engineering, University of Ulsan, 93 Daehakro, Namgu, Ulsan 680-749,  
Republic of Korea*

*<sup>3</sup>Department of Physics, National Institute of Technology, Hazratbal, Srinagar-190006, India*

*<sup>4</sup>Department of Physics, LNM Institute of Information Technology, Jaipur-302031, India*

*\*Corresponding authors*

Jin Suk Chung; Email: jschung@mail.ulsan.ac.kr, Tel: +82-52-259-2249, Fax: +82-52-259-1689.

## [ESI-1] Synthesis of graphene oxide

Expandable graphite (Grade 1721) was obtained from Asbury Carbon (USA). Potassium permanganate (KMnO<sub>4</sub>), hydrochloric acid (HCl), hydrogen peroxide (H<sub>2</sub>O<sub>2</sub>) and silver nitrate were purchased from Sigma Aldrich (USA). Titanium (IV) chloride and ethanol (Analytical grade) were obtained from Merck (USA).

Graphene oxide (GO) was synthesized from natural graphite powders using a modified Hummer's method. In a typical process, 7 g of graphite was charged into a 1 L beaker and heated for 10 seconds in a microwave oven; this step expanded the graphite to 150–200 times of its original volume. The resulting graphite was dispersed in concentrated H<sub>2</sub>SO<sub>4</sub> (1000 mL) at ~0°C with continuous stirring. Then, 42 g of KMnO<sub>4</sub> was slowly added at a temperature not to exceed 20°C. The temperature was then elevated to 35°C and the suspension was stirred for 2 h. The flask was then chilled again in the ice bath, and distilled water (ice) was slowly added, maintaining the temperature below 70°C. The mixture was stirred for 1 h and subsequently diluted with 5 L of deionized water. Subsequently, 50 mL of H<sub>2</sub>O<sub>2</sub> (30 wt %) was added and vigorous bubbles appeared as the color of the suspension changed from dark brown to yellow. The suspension was centrifuged and washed four times with 10% HCl solution, followed by centrifuging at 10000 rpm and washing with deionized water through four centrifuge cycles to completely remove the acid until the pH of the GO dispersion reached 6. At this point, the as-synthesized GO dispersion was a paste. The concentration of GO was 0.91 wt%, as determined after drying the GO dispersion at 100°C in an oven for 24 hours.

## [ESI-2] Synthesis of Ti<sub>y</sub>Ag<sub>(1-y)</sub>O<sub>2</sub>, (where y = 1.0, 0.08, 0.06, 0.04, 0.02)

For synthesis of Ag-doped TiO<sub>2</sub> nanoparticles, 3 grams of silver nitrate was dissolved in a beaker containing a 100 ml mixture of ethanol and water in a ratio of 60:40 (60 ml ethanol and 40 ml water). Subsequently, this Ag liquid solution was ultrasonicated for 30 minutes. Thus, the solution was ready to use and a different amount/volume of this solution was used for varying the amount of dopant (Ag) (different value of y) in the Ti<sub>y</sub>Ag<sub>(1-y)</sub>O<sub>2</sub> series nanomaterials.

**ESI-2.1. Synthesis of pure TiO<sub>2</sub>, (here y = 1.0):** For preparation of the pure titanium oxide material, 50 ml of ethanol was used as a solvent and then 20 ml of titanium (IV) chloride was slowly-added drop-wise to ethanol. The reaction was performed at room temperature on a magnetic stirrer inside a fume hood as a large amount of Cl<sub>2</sub> and HCl gases were released during

the reaction. After the reaction, the whole solution is a non-homogenous solution, with a small amount of yellowish liquid on the bottom of the beaker and foam-like yellow gel on top. To make the solution uniform and homogenous, distilled water was added drop-wise, resulting in a milky color solution as  $\text{Cl}_2$  and  $\text{HCl}$  gases evolved in the reaction. A pH of 1 was maintained in all the cases before adding water to the solution. As the gas evolution ceased, the resulting milky gel was allowed to cool to room temperature (because the temperature of the solution increased during the reaction) to ensure that there was no unreactive material in the gel-solution. The obtained gel was further dried in the same magnetic stirrer for 4 hours at  $100^\circ\text{C}$ . The obtained material was crushed to produce a powder, which was further calcined for 4 hours in a box furnace at  $400^\circ\text{C}$  to produce the pure anatase phase of the  $\text{TiO}_2$  nanoparticles. Temperatures greater than this were not tested because at higher temperature, the anatase phase converts into an anatase-rutile mixed phase. This sample is identified as **ATO-(0)** for simplicity and identification purpose.

**ESI-2.2. Synthesis of  $\text{Ti}_{0.08}\text{Ag}_{0.02}\text{O}_2$ , (here  $y = 0.08$ ):** For preparation of  $\text{Ti}_{0.08}\text{Ag}_{0.02}\text{O}_2$ , 50 ml of ethanol was used as a solvent and 19.6 ml of titanium (IV) chloride was added slowly drop wise to ethanol and  $\sim 6.7$  ml of Ag solution (as discussed above) was added. At this stage, the whole solution is a non-homogenous solution, with a small amount of yellowish liquid on the bottom of beaker and foam-like yellow gel on top. To make the solution uniform and homogenous, distilled water was added drop-wise, resulting in a milky color of the solution due to the further release of  $\text{Cl}_2$  and  $\text{HCl}$  gases from the reaction. As the gas evolution ceased, the resulting white gel was allowed to cool to room temperature (because the temperature of the solution increased during the reaction) to ensure that there was no unreactive material in the gel-solution. The obtained gel was further dried using the same magnetic stirrer for 4 hours at  $100^\circ\text{C}$ . The obtained material was crushed to produce a powder and the powder sample was further calcined for 4 hours in a box furnace at  $400^\circ\text{C}$ . This sample is identified as **ATO-(1)**.

**ESI-2.3. Synthesis of  $\text{Ti}_{0.06}\text{Ag}_{0.04}\text{O}_2$ , (here  $y = 0.06$ ):** The whole process was similar to as discussed in **Section 2.2**, but here 19.2 ml of titanium (IV) chloride and  $\sim 13.4$  ml of the Ag solution (as discussed above) were used for the reaction. This sample is identified as **ATO-(2)**.

**ESI-2.4. Synthesis of  $\text{Ti}_{0.04}\text{Ag}_{0.06}\text{O}_2$ , (here  $y = 0.04$ ):** The whole process was similar to as discussed in **Section 2.2**, but 18.8 ml of titanium (IV) chloride and  $\sim 20.1$  ml of the Ag solution (as discussed above) were used for the reaction. This sample is identified as **ATO-(3)**.

**ESI-2.5. Synthesis of  $\text{Ti}_{0.02}\text{Ag}_{0.08}\text{O}_2$ , (here  $y = 0.02$ ):** The whole process is similar to as discussed in **Section 2.2**, but 18.4 ml of titanium (IV) chloride and ~ 26.8 ml of the Ag solution (as discussed above) were used for the reaction. This sample is identified as **ATO-(4)**.

### **[ESI-3] Synthesis of graphene/ $\text{Ti}_y\text{Ag}_{(1-y)}\text{O}_2$ hybrid materials**

After preparation of ATO-(0), ATO-(1), ATO-(2), ATO-(3), and ATO-(4) samples, 0.1 gram from each sample was dissolved in 250 ml of ethanol in five different beakers under magnetic stirring and then ultrasonicated for 30 minutes. For synthesis of graphene/ $\text{Ti}_y\text{Ag}_{(1-y)}\text{O}_2$  hybrid materials, 3 grams of GO was dissolved in 250 ml of ethanol followed by magnetic stirring and then ultrasonication for 30 minutes. 50 ml of the completely dispersed GO solution was added to each of the five beakers and then ultrasonicated for 30 minutes at 50<sup>0</sup>C. The homogenous suspensions of all samples were centrifuged at 8000 rpm at 10<sup>0</sup>C. All the samples were then dried at 70<sup>0</sup>C for 24 hours in an oven and then ground in a pastel mortar to produce a fine homogenous powder of graphene-incorporated  $\text{Ti}_y\text{Ag}_{(1-y)}\text{O}_2$  materials. All the powder samples were annealed in a tubular furnace at 400<sup>0</sup>C with a heating rate of 10<sup>0</sup>C/minute for 4 hours in the presence of a N<sub>2</sub> gas atmosphere. Thus, all the samples synthesized were renamed as GATO-(0), GATO-(1), GATO-(2), GATO-(3), and GATO-(4) for simplicity in comparisons and identification purposes. The carbonyl, carboxyl, and hydroxyl functional groups on graphene sheets act as heterogeneous nucleation sites for Ag-doped TiO<sub>2</sub> nanostructures, which results in the formation of well-dispersed polycrystalline TiO<sub>2</sub> nanostructures on the graphene sheets.

**ESI-3.1. Synthesis of graphene/TiO<sub>2</sub>:** This sample is named as **GATO-(0)**.

**ESI-3.2. Synthesis of graphene/Ti<sub>0.08</sub>Ag<sub>0.02</sub>O<sub>2</sub>:** This sample is named as **GATO-(1)**.

**ESI-3.3. Synthesis of graphene/Ti<sub>0.06</sub>Ag<sub>0.04</sub>O<sub>2</sub>:** This sample is named as **GATO-(2)**.

**ESI-3.4. Synthesis of graphene/Ti<sub>0.04</sub>Ag<sub>0.06</sub>O<sub>2</sub>:** This sample is named as **GATO-(3)**.

**ESI-3.5. Synthesis of graphene/Ti<sub>0.02</sub>Ag<sub>0.08</sub>O<sub>2</sub>:** This sample is named as **GATO-(4)**.

[ESI-4]. Rietveld refinement of X-ray diffraction (XRD) pattern:-

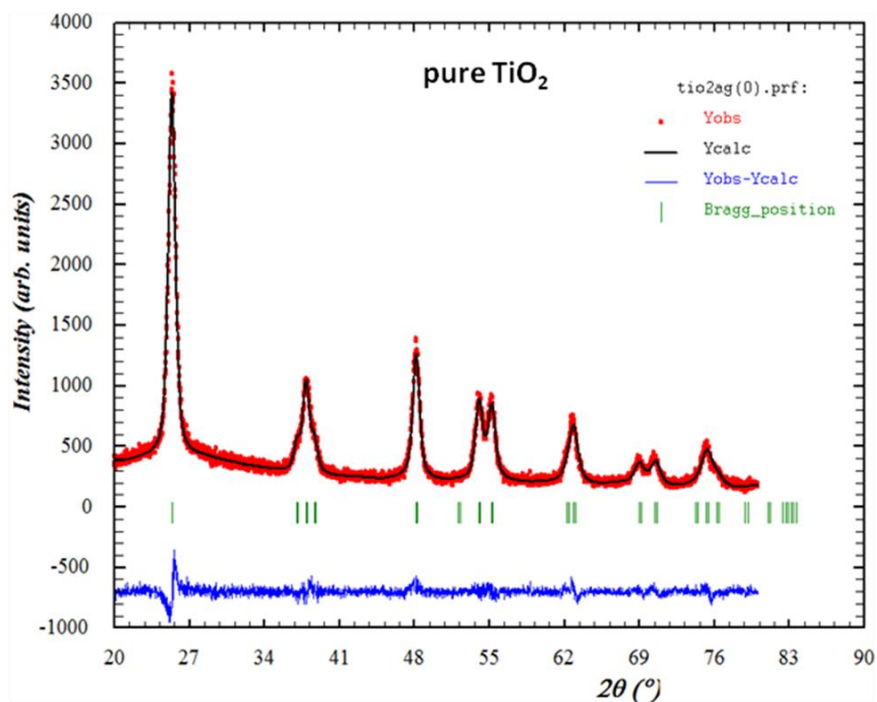


Figure S-1. X-ray diffraction patterns and FULLPROOF based Rietveld refinement of X-ray diffraction (XRD) pattern of ATO-(0) sample.

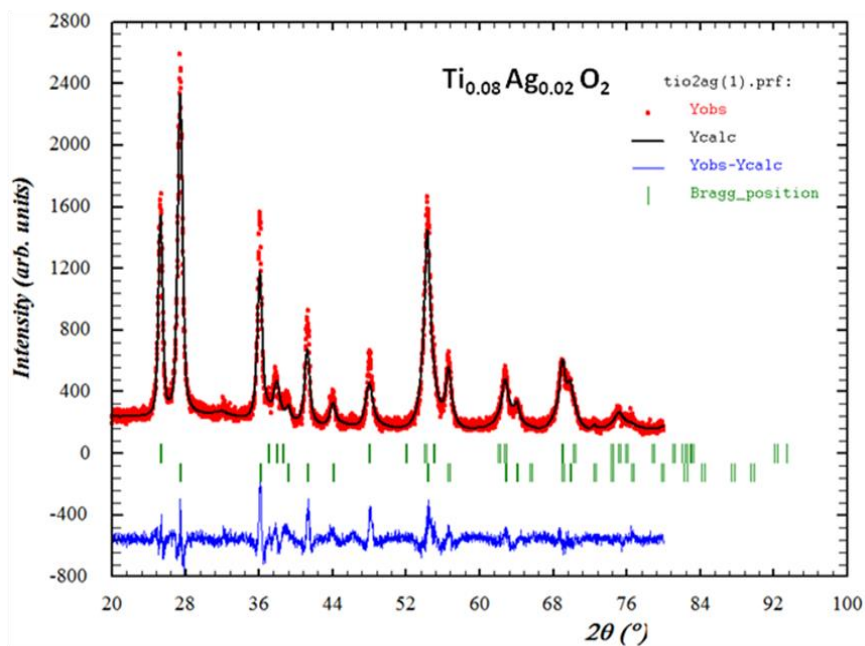


Figure S-2. X-ray diffraction patterns and FULLPROOF based Rietveld refinement of X-ray diffraction (XRD) pattern of ATO-(1) sample.

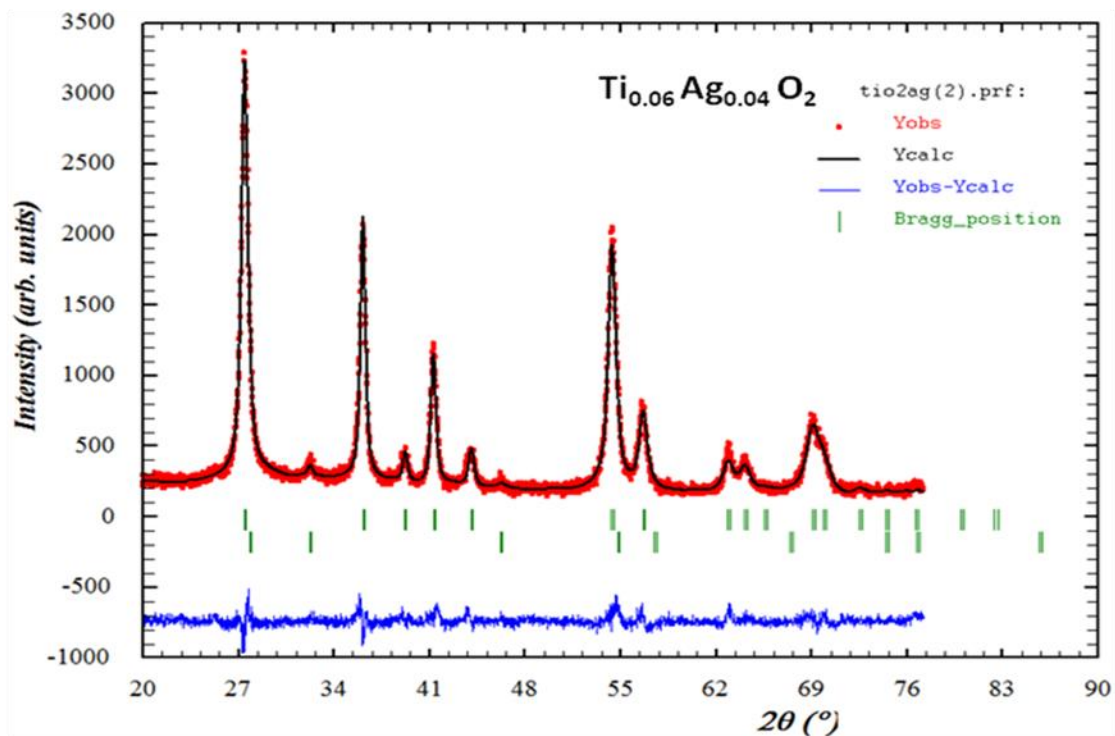


Figure S-3. X-ray diffraction patterns and FULLPROOF based Rietveld refinement of X-ray diffraction (XRD) pattern of ATO-(2) sample.

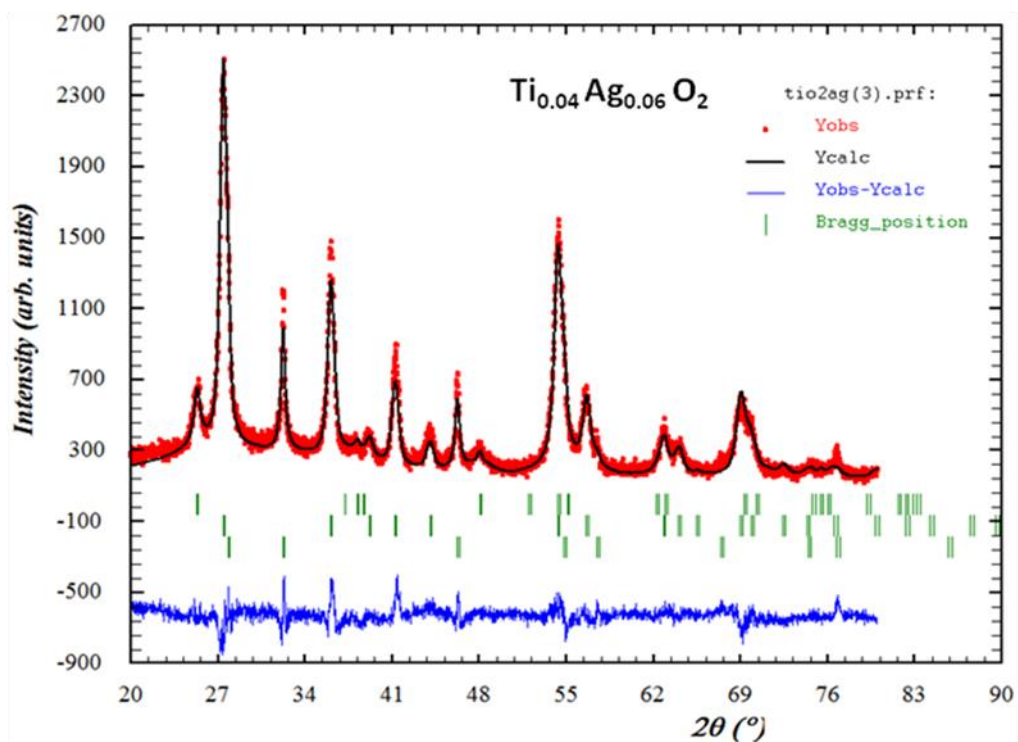


Figure S-4. X-ray diffraction patterns and FULLPROOF based Rietveld refinement of X-ray diffraction (XRD) pattern of ATO-(3) sample.

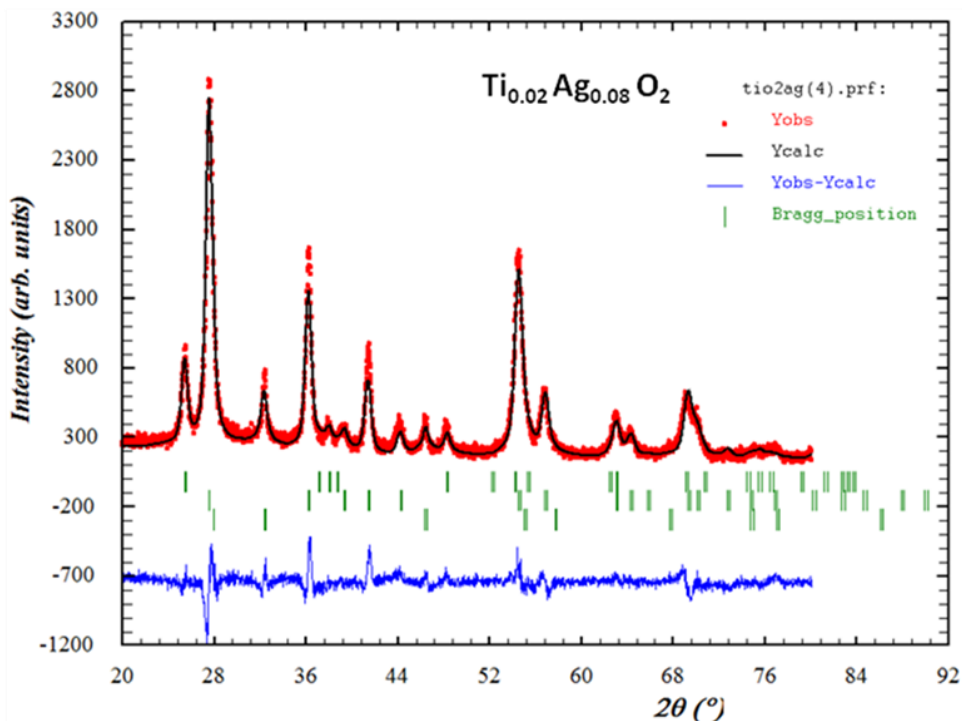


Figure S-5. X-ray diffraction patterns and FULLPROOF based Rietveld refinement of X-ray diffraction (XRD) pattern of ATO-(4) sample.

[ESI-5]. FULLPROOF based structural Rietveld refinement parameters:

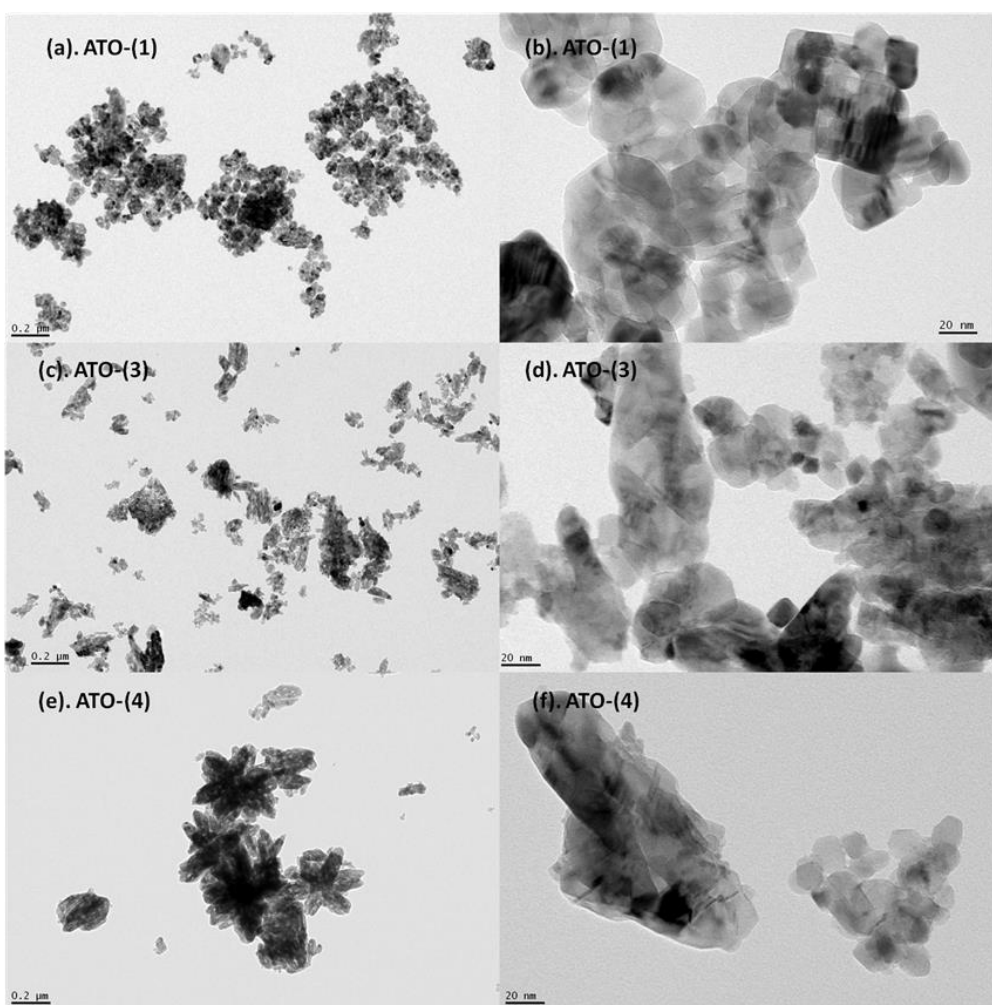
Table 1. Rietveld analysis for XRD pattern of prepared Ag doped TiO<sub>2</sub> nanoparticles.

Sample name	Phase name	a = b (Å)	c (Å)	atom name	x	y	z	B	u	v	w	IG	R <sub>p</sub>	R <sub>wp</sub>	R <sub>exp</sub>	χ <sup>2</sup>
ATO-(0)	anatase	3.776	9.492	Ti	0	0.75	0.125	2.07	5.47	-4.33	.912	.399	16.3	15.8	10.4	2.29
				O	0	0.75	0.333	1.48								
ATO-(1)	anatase	3.791	9.486	Ti	0	0.75	0.125	-6.48	-3.2	3.56	-2.51	2.07	18.2	20.3	9.59	4.5
				O	0	0.75	0.341	-13.9								
				Ag	0	0.75	0.125	-6.48								
	rutile	4.596	2.959	Ti	0	0	0	-0.08	0.92	-0.32	0.34	0.07				
O	0.299	0.299	0	-1.98												
Ag	0	0	0	-0.08												
ATO-(2)	rutile	4.593	2.955	Ti	0	0	0	9.317	8.53	-6.85	0.39	1.01	15.4	16	9.95	2.59
				O	0.298	0.298	0	6.787								
				Ag	0	0	0	9.317								
	AgCl	5.552	5.552	Ag	0	0	0	52.07	-5.9	7.29	-1.18	-0.11				
Cl	0.5	0.453	0.453	86.51												
ATO-(3)	anatase	3.786	9.422	Ti	0	0.75	0.125	41.30	0.93	-0.32	0.34	0.07	19.4	20.9	10.8	3.71
				O	0	0.75	0.339	29.86								
				Ag	0	0.75	0.125	41.30								
	rutile	4.595	2.958	Ti	0	0	0	5.519	0.93	-0.32	0.34	0.07				
				O	0.301	0.301	0	2.148								
				Ag	0	0	0	5.519								
AgCl	5.5497	5.5497	Ag	0	0	0	47.99									
Cl	0.5	0.334	0.334	-41.8												
ATO-(4)	anatase	3.767	9.472	Ti	0	0.75	0.125	3.051	0.93	-0.32	0.34	0.07	20.2	21.6	10.4	4.3
				O	0	0.75	0.916	-2.37								
				Ag	0	0.75	0.125	3.051								
	rutile	4.5792	2.9487	Ti	0	0	0	6.741	0.93	-0.32	0.34	0.07				
				O	0.299	0.299	0	3.069								
				Ag	0	0	0	6.741								
AgCl	5.5315	5.5315	Ag	0	0	0	57.65	0.93	-0.32	0.34	0.07					
Cl	0.5	0.333	0.333	-28.2												

Where; a, b, c = lattice constant; x, y, z, B = Wyckoff positions; u, v, w, IG = FWHM parameter; ( $R_p$ ) = profile residual factor; ( $R_{wp}$ ) = weighted profile residual error; ( $R_{exp}$ ) = expected pattern factor;  $\chi^2$  = goodness of fitting.

### [ESI-6]. TEM for Ag doped TiO<sub>2</sub> series:

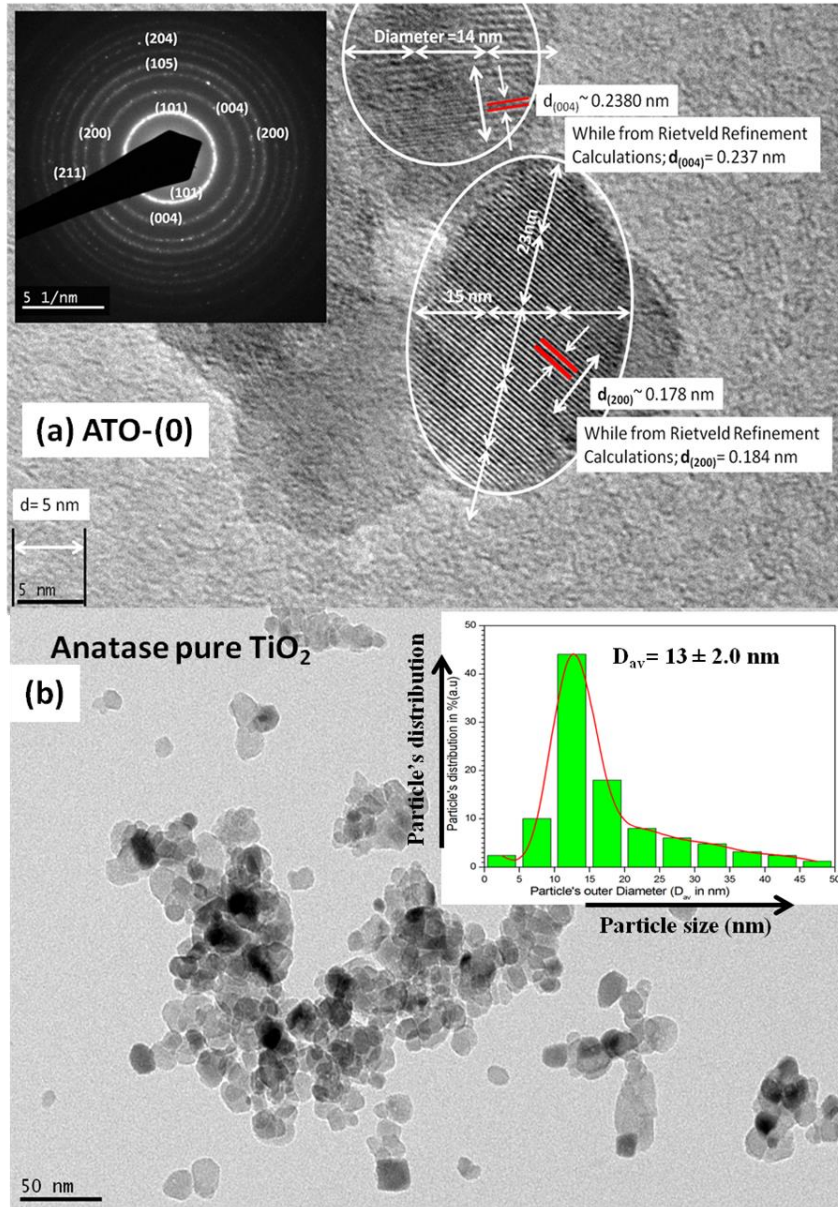
From TEM images, it is clear that the nanoparticles size is varying with the increase of Ag doping in host material while the reaction time, temperature and other environmental conditions was kept same in all the cases.

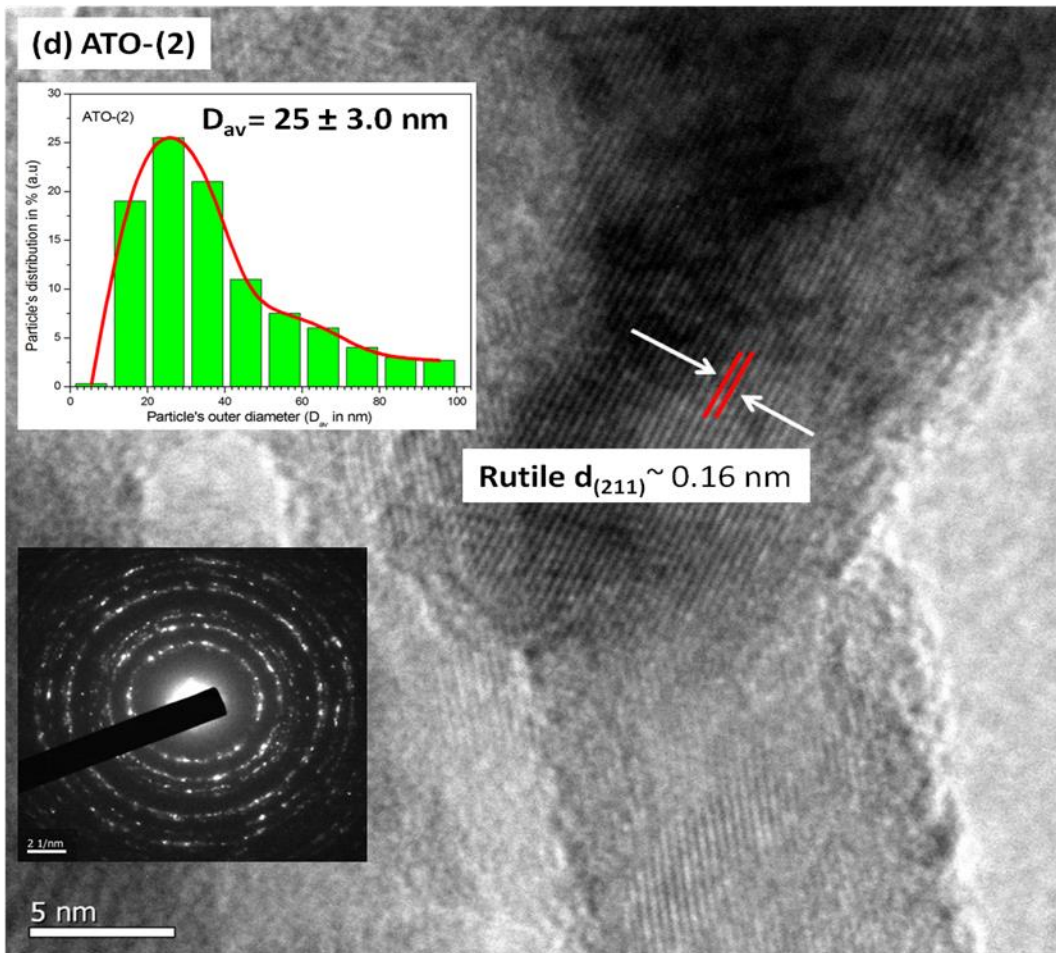
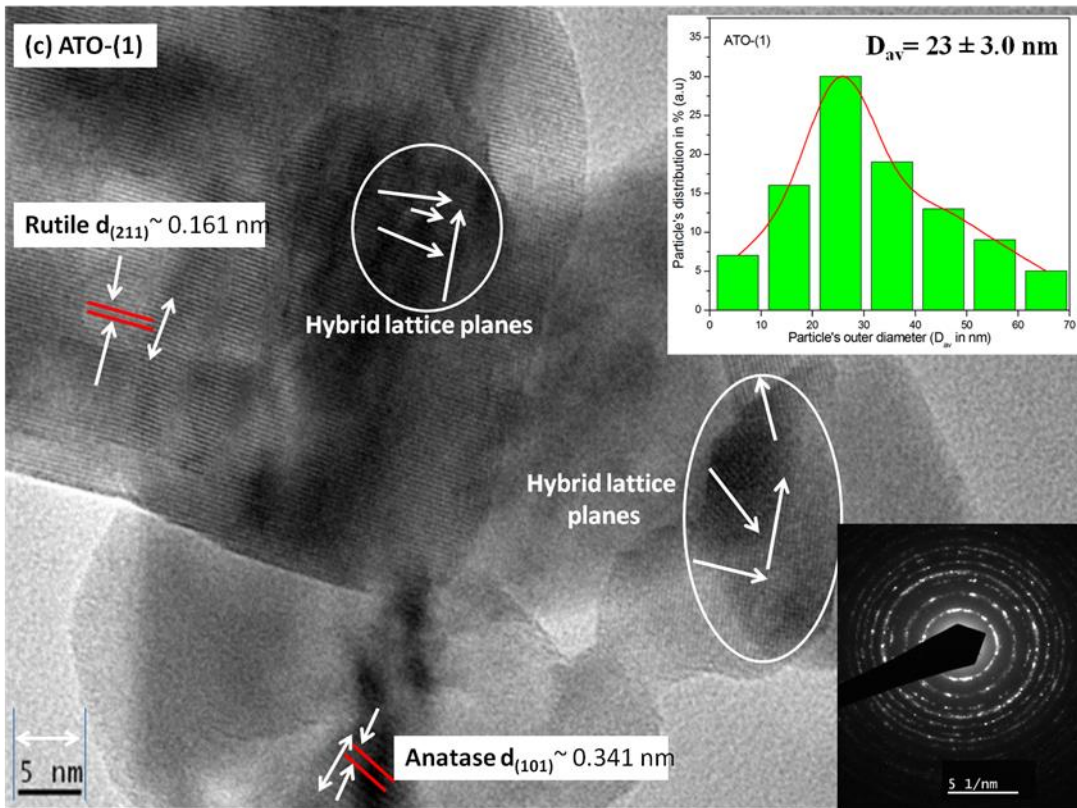


**Figure S-6. Transmission Electron Microscopy (TEM) for Ag doped TiO<sub>2</sub> series at different scale: (a) ATO-(1) sample at 0.2 μm scale; (b) ATO-(1) sample at 20 nm scale; (c) ATO-(3) sample at 0.2 μm scale; (d) ATO-(3) sample at 20 nm scale; (e) ATO-(4) sample at 0.2 μm scale; (f) ATO-(4) sample at 20 nm scale.**

# [ESI-7]. HRTEM, SAED, and particle size distribution curve of Ag doped TiO<sub>2</sub> nanoparticles:

HRTEM observation shown here are to provide an insight into the structural and morphological characteristics of sample ATO-(0), ATO-(1), ATO-(2), ATO-(3), and ATO-(4) respectively.





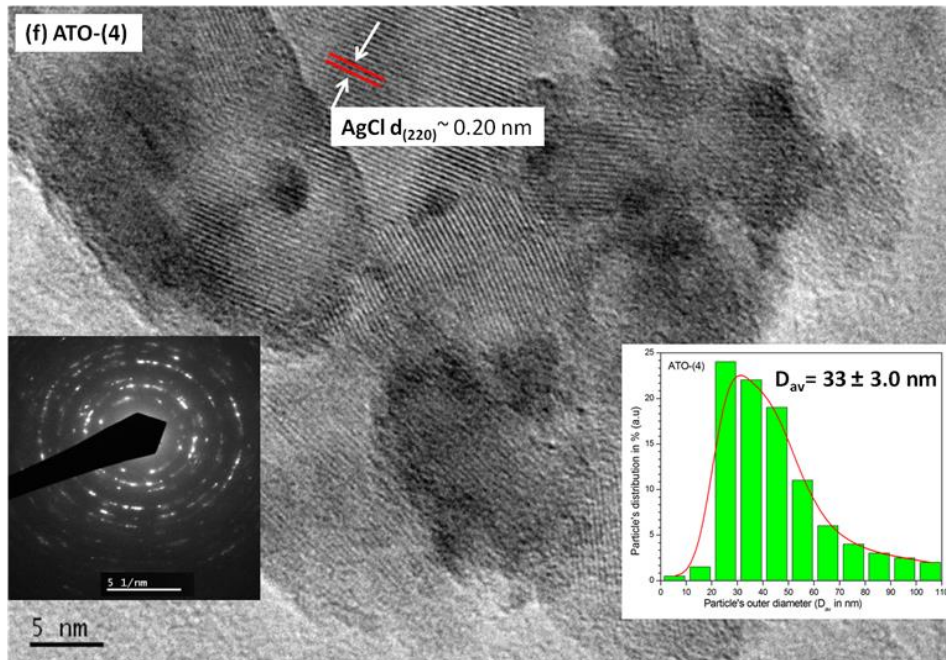
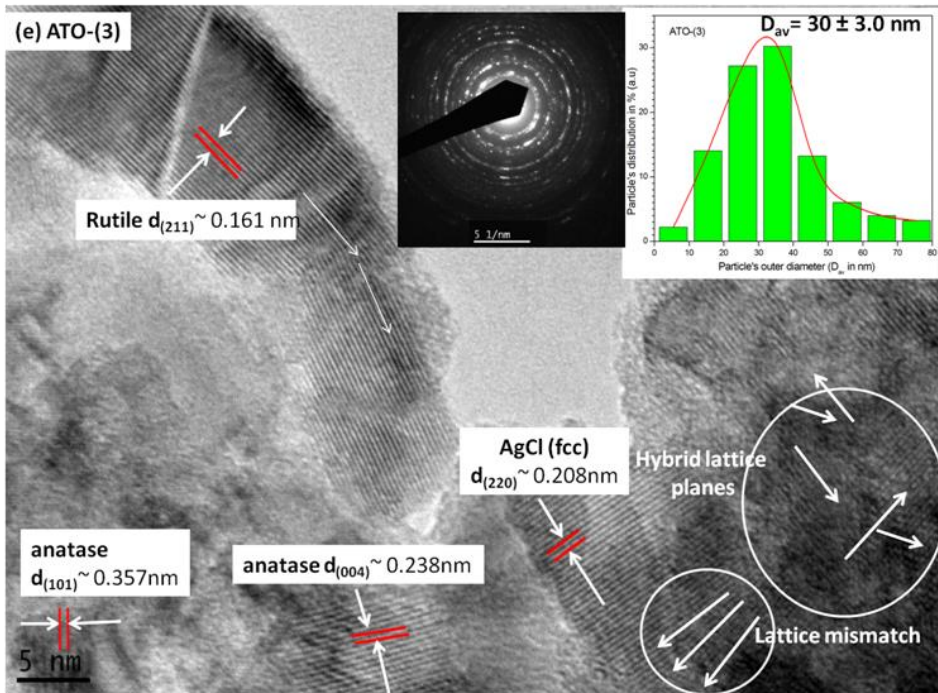
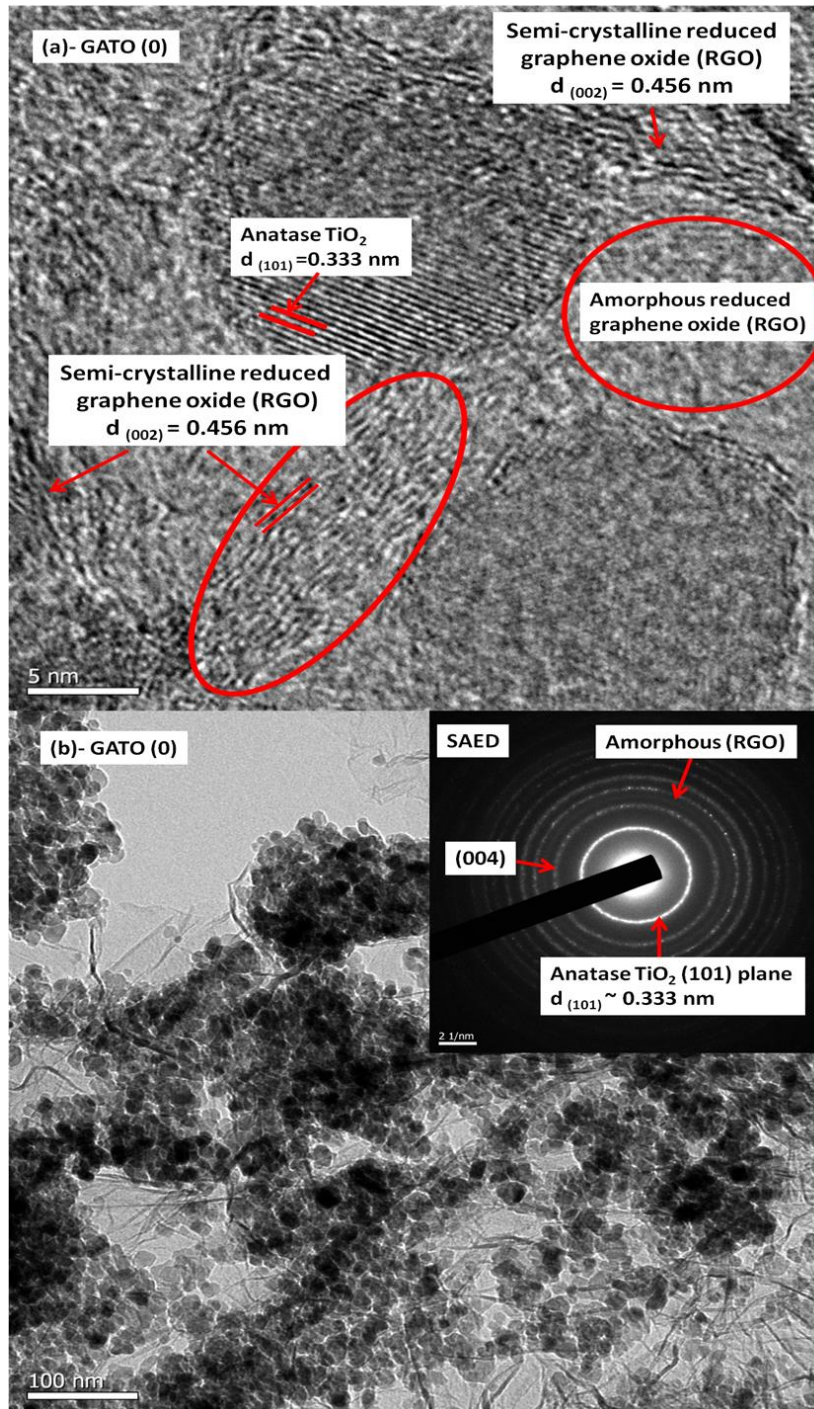
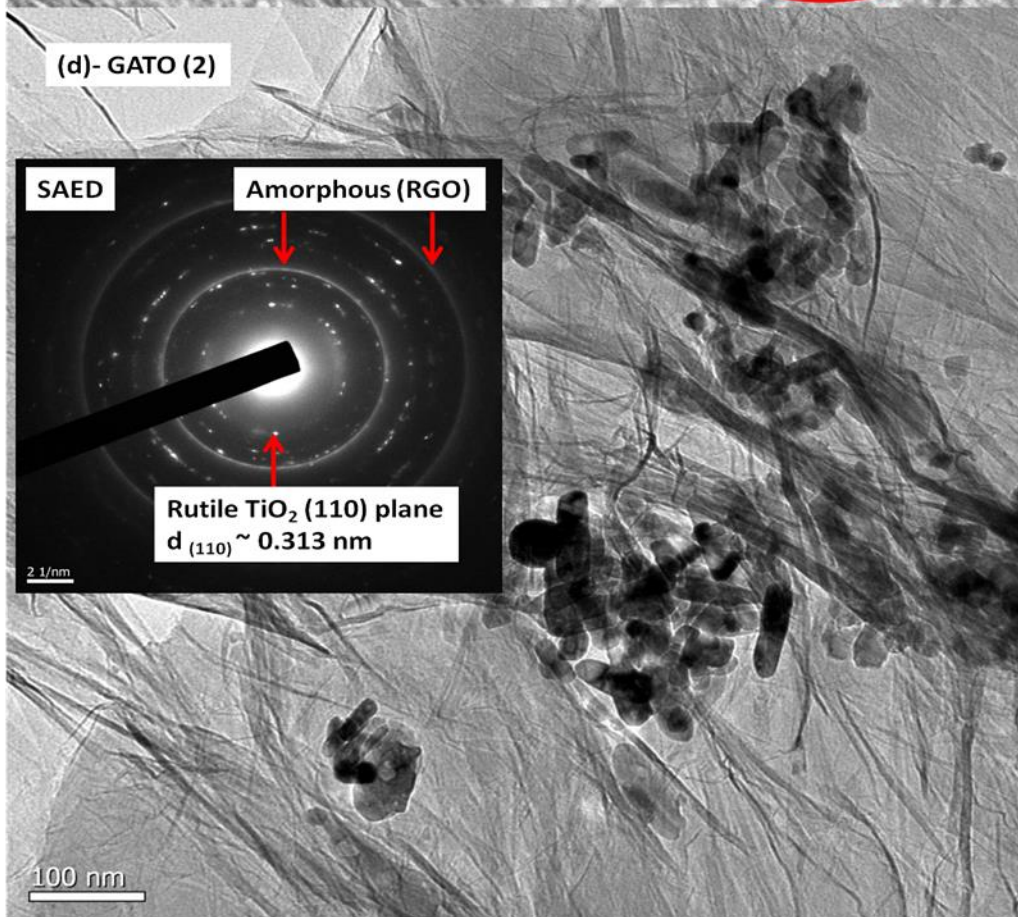
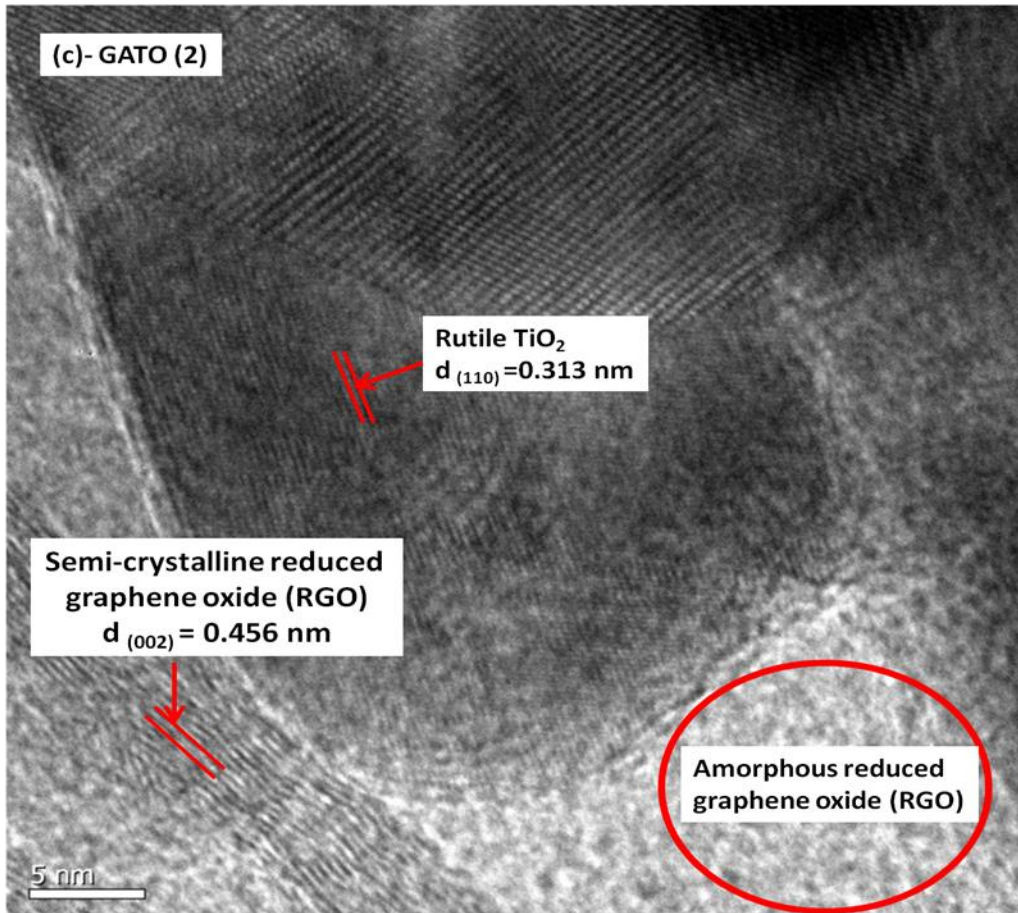
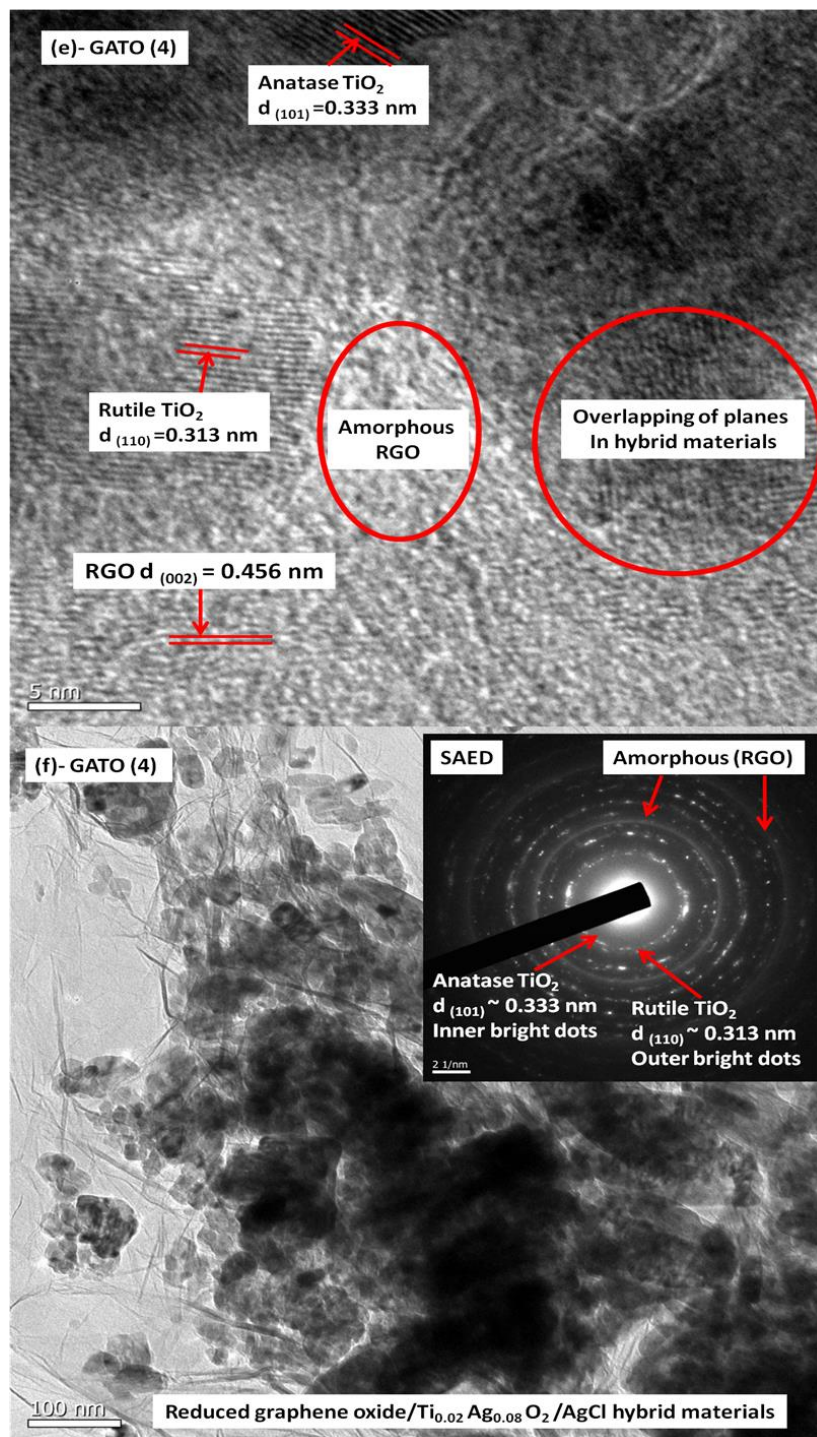


Figure S-7. HRTEM, SAED, and particle size distribution curve for Ag doped  $\text{TiO}_2$ : (a) ATO-(0) sample at 5 nm scale, and inset shows SAED pattern with diffraction planes of anatase  $\text{TiO}_2$ ; (b) ATO-(0) sample at 50 nm scale and in inset the corresponding particle size distribution graph; (c) ATO-(1) sample at 5 nm scale and inset shows SAED pattern, and particle size distribution graph; (d) ATO-(2) sample at 5 nm scale and inset shows SAED pattern, and particle size distribution graph; (e) ATO-(3) sample at 5 nm scale and inset shows SAED pattern, and particle size distribution graph; (f) ATO-(4) sample at 5 nm scale and inset shows SAED pattern, and particle size distribution graph.

**[ESI-8]. FETEM and SAED images of reduced graphene oxide decorated Ag doped TiO<sub>2</sub> (Ti<sub>y</sub> Ag<sub>(1-y)</sub> O<sub>2</sub>/AgCl hybrid system) nanoparticles:** Field Emission Transmission Electron Microscopy (FETEM) observation shown here are to provide an insight into the structural and morphological characteristics of sample GATO-(0), GATO-(2), and GATO-(4) respectively. The rings corresponding to amorphous reduced graphene oxide was clearly distinguished from the diffraction pattern of Ag-doped TiO<sub>2</sub> nanostructures.







**Figure S-8. FETEM, SAED, for graphene decorated Ag doped  $\text{TiO}_2$ : (a) GATO-(0) sample at 5 nm scale, (b) GATO-(0) sample at 100 nm scale and inset shows SAED pattern, (c) GATO-(2) sample at 5 nm scale, (d) GATO-(2) sample at 100 nm scale and inset shows SAED pattern, (e) GATO-(4) sample at 5 nm scale, (f) GATO-(4) sample at 100 nm scale and inset shows SAED pattern of hybrid  $\text{TiO}_2$  materials.**

**ESI-8. NOTE:** HRTEM, FETEM are an important tool for analysis of texture and identification of the phases present in the materials. If one knows the camera constant ( $L\lambda$ ) then calculation of interplanar distance {by using the expression:  $rd_{hkl} = L\lambda$ ,  $L$  -camera length,  $r$  -distance between transmitted (centre spot) and diffracted spots (bright spots in the concentric ring),  $d_{hkl}$  - interplanar distance ( $\text{\AA}$ )} can be done easily by measuring bright spotted ring diameters (then  $r =$  half of the distance between two bright spot in a ring passing through the transmitted (centre spot) in SAED image. This is due to fact that the all diffraction spots are obtained from planes belonging to one zone of Ewald sphere in reciprocal lattice plane and thus reciprocal lattice becomes a series of rings (circles in two dimensions) concentric with the origin of the reciprocal lattice. It is evident from SAED image of ATO-(1), ATO-(2), ATO-(3), and ATO-(4) samples that it is difficult to identify all the planes (as few of the bright spot overlap with each other) of hybrid structure due to multi phase (anatase/rutile/ FCC AgCl) polycrystalline nature of the samples as rings are constituted of a collection of spots of the different nanocrystal orientations.

**[ESI-9]. Tauc plot of UV-Vis absorption spectrum:**

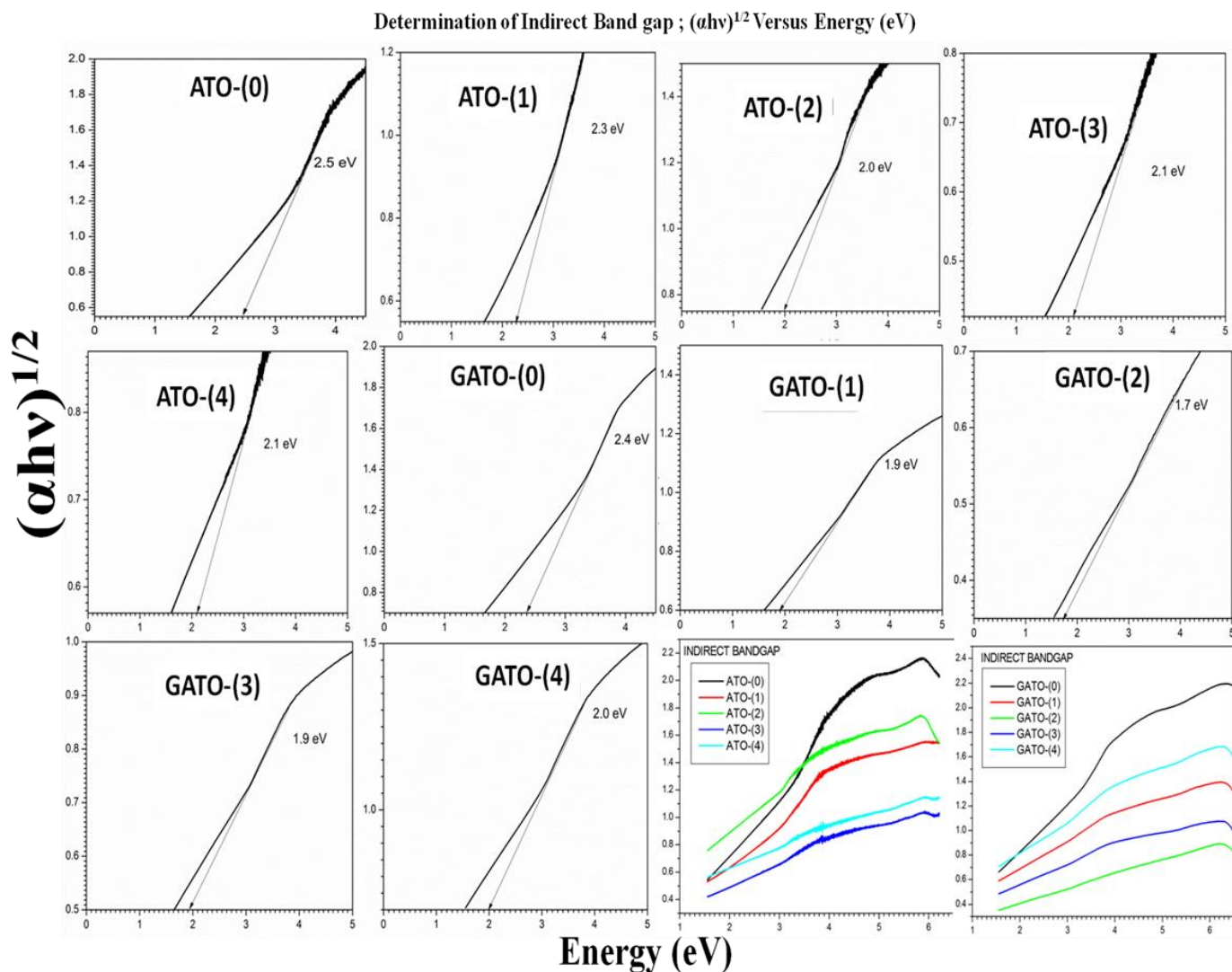


**Figure S-9. Tauc plot for determination of Indirect band gap of all samples.**

Determination of Direct Band gap ;  $(\alpha h\nu)^2$  Versus Energy (eV)

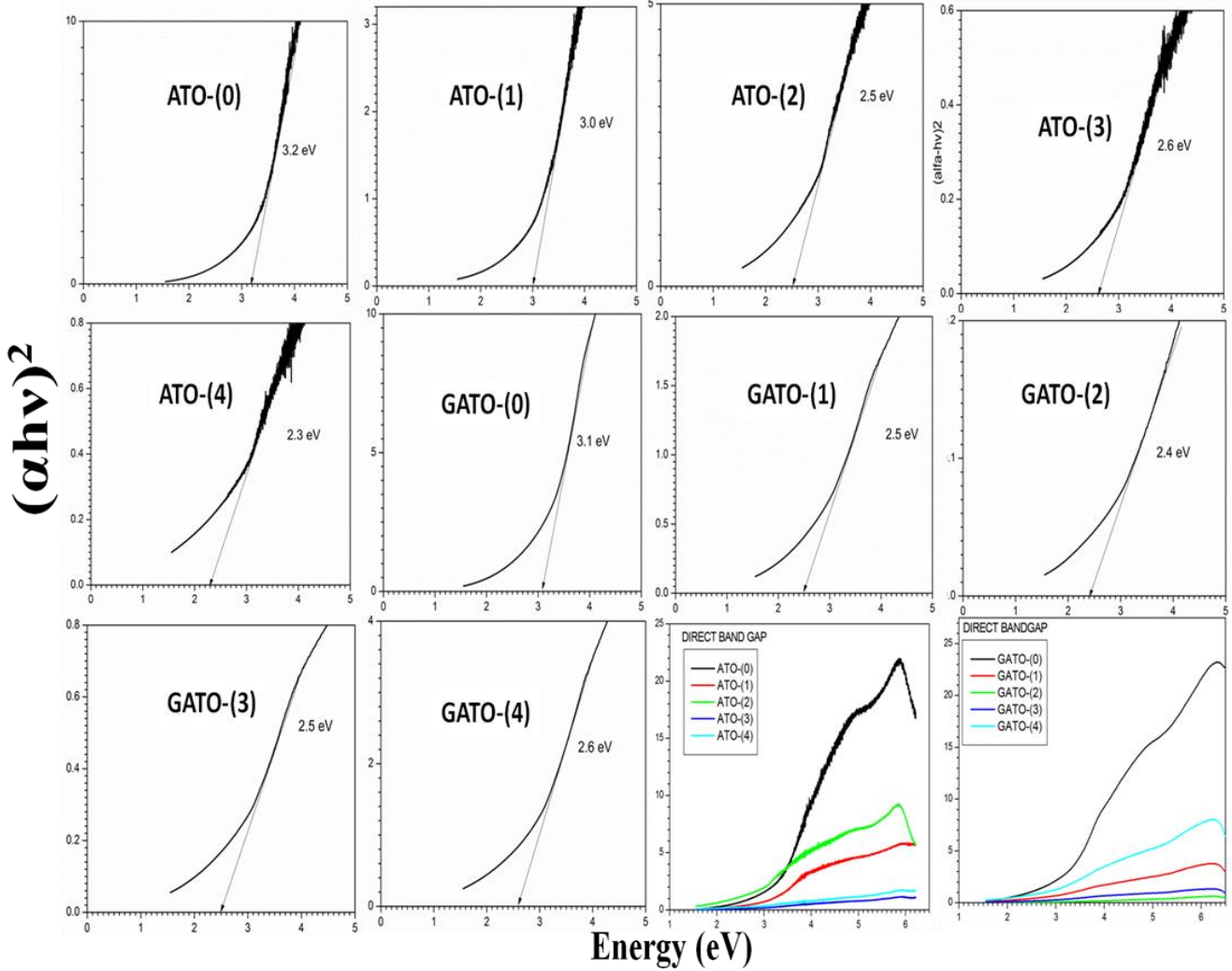


**Figure S-10. Tauc plot for determination of direct band gap of all samples.**

The variation in the band gap for a direct transition ( $\Gamma-\Gamma$  transition) are apparently higher than the observed in an indirect transition ( $\Gamma-L$  /  $M-\Gamma$  / or any other transition for different phases) for ATO-(3), ATO-(4), GATO-(3) and GATO-(4) samples. This is due to fact of an additional fcc AgCl crystal that has an indirect transition ( $\Gamma-L$  transition) of 3.28 eV while a direct transition ( $\Gamma-\Gamma$  transition) of 5.28 eV. The blue shift has also been observed in graphene decorated doped  $\text{TiO}_2$  hybrid nanostructures for  $\text{Ti}_{0.02}\text{Ag}_{0.08}\text{O}_2$  sample. Most probably, the blue shift in the absorption spectrum (direct transition of GATO-(4)) may be due to the increasing surface plasmon frequency of the free electron gas on the surface of graphene sheet. It is due to fact that the electron density increases due to transfer of larger number of electrons from conduction band of hybrid materials (from Ag doped  $\text{TiO}_2/\text{AgCl}$ ) to the graphene sheet. In addition to this, there is a possibility of shift in Fermi levels since the Fermi level of metals such

as Ag is more positive than the conduction band of TiO<sub>2</sub>, so that the photogenerated electrons can transfer to Ag nanoparticles. If the electrons remain stored within the Ag nanoparticles, then the Fermi level shifts towards more negative potentials as well as increasing the surface plasmon frequency [S1]. It is further the subject of detail investigations but right now it is beyond the scope of this paper.

### [ESI-10]. FTIR transmittance spectra analysis:

**Table 2: The main peak and dip positions for various bond stretching modes observed in FTIR spectrum.**

Sample name	Peak position cm <sup>-1</sup> & bond name	Dip position cm <sup>-1</sup> & bond name	Dip position cm <sup>-1</sup> & bond name	Dip position cm <sup>-1</sup> & bond name	Peak position cm <sup>-1</sup> & bond name
<b>ATO-(0)</b>	1126.28 cm <sup>-1</sup> (Ti-O-Ti) stretching	1226.56 cm <sup>-1</sup> , (O-H) deformation	1635.42 cm <sup>-1</sup> , (O-H)	3421.269cm <sup>-1</sup> , (O-H) stretching	3651.56 cm <sup>-1</sup> (Ti-OH)
<b>ATO-(1)</b>	1141.709, (Ti-O-Ti)	1226.56, (O-H)	1635.42, (O-H)	nil	nil
<b>ATO-(2)</b>	1106.995, (Ti-O-Ti)	nil	1627.706, (O-H)	nil	nil
<b>ATO-(3)</b>	1091.566, (Ti-O-Ti)	nil	1646.992, (O-H)	nil	3752.98,(Ti-OH)
<b>ATO-(4)</b>	1110.852, (Ti-O-Ti)	nil	1627.706, (O-H)	nil	nil
<b>GATO-(0)</b>	1020.209, (Ti-O-C)	1230.42, (O-H)	1585.28,(O-H) RGO	nil	3590.76,(Ti-OH)
<b>GATO-(1)</b>	1016.352, (Ti-O-C)	1222.71, (O-H)	1575.64,(O-H) RGO	nil	nil
<b>GATO-(2)</b>	1016.352, (Ti-O-C)	1222.71, (O-H)	1558.28,(O-H) RGO	nil	nil
<b>GATO-(3)</b>	1004.781, (Ti-O-C)	1230.42, (O-H)	1608.42,(O-H) RGO	nil	3455.98,(Ti-OH)
<b>GATO-(4)</b>	1012.495, (Ti-O-C)	1230.42, (O-H)	1616.14,(O-H) RGO	nil	nil

### [ESI-11]. Basic Information about FESEM, EDX Analysis:

**Note.** Platinum (Pt) coating was done on all the samples to make the sample surface conducting, so we can see a peak corresponding to Pt also in EDX spectra of all the samples as shown in the EDX spectrum of the manuscript.

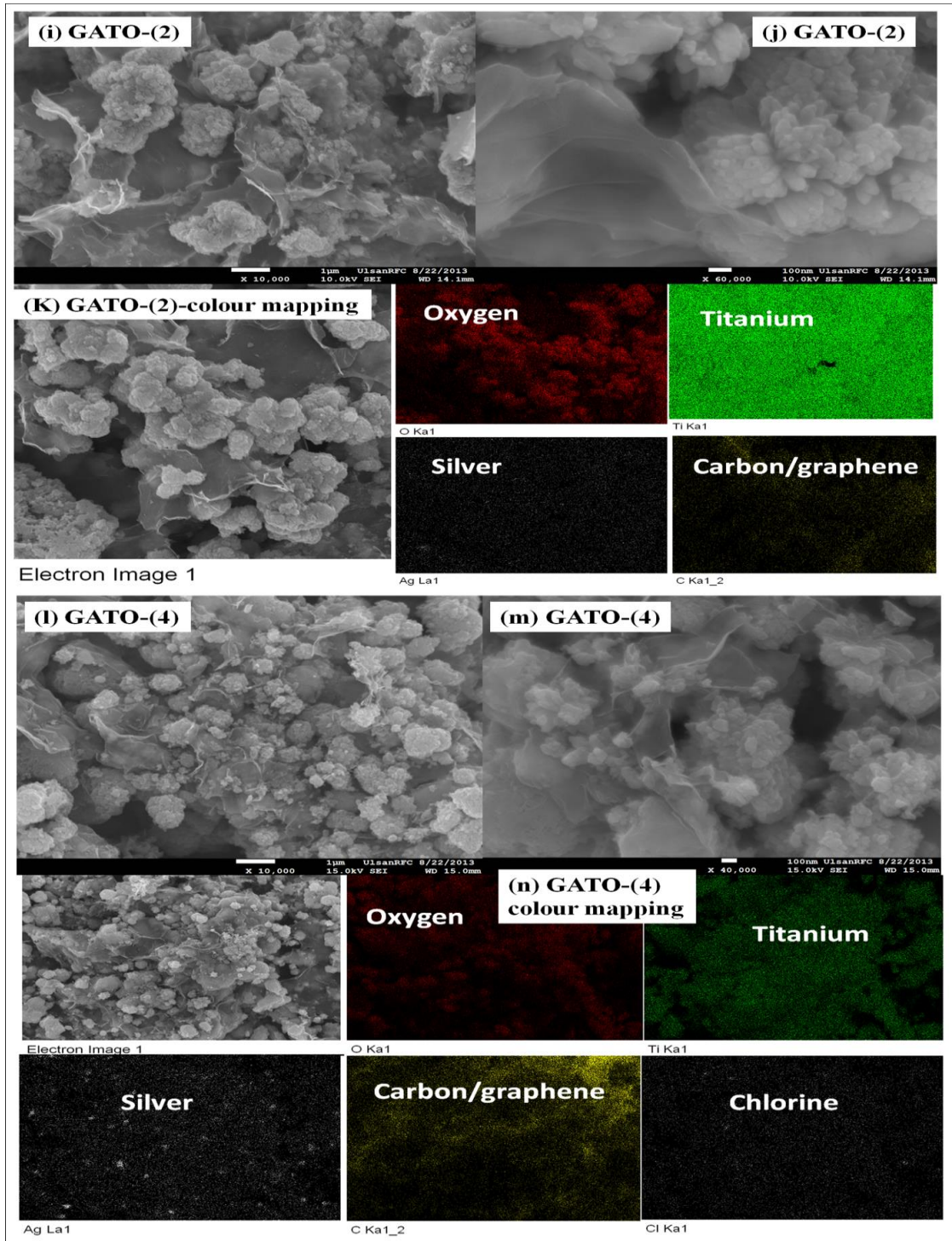


**Figure S-11. Field Emission Scanning Electron Microscopy (FESEM), Color mapping micrographs (i) GATO-(2) sample at 1  $\mu\text{m}$  scale; (j) GATO-(2) sample at 100 nm scale; (k) area selected for the color mappings of GATO-(2) sample and color mapping images of the elements present in the sample. (l) GATO-(4) sample at 1  $\mu\text{m}$  scale; (m) GATO-(4) sample at 100 nm scale; (n) area selected for the color mappings of GATO-(4) sample and color mapping images of the elements present in the sample.**

## [ESI-12]. Raman band observed in Raman spectrum:

**Table 3. The main peak positions for various Raman bands observed in case of all samples.**

Sample name versus band name & position	Peak position in $\text{cm}^{-1}$ & band name (Eg)-TiO <sub>2</sub>	Peak position in $\text{cm}^{-1}$ & band name (A1g +B1g)	Peak position in $\text{cm}^{-1}$ & band name (B1g)- TiO <sub>2</sub>	Peak position in $\text{cm}^{-1}$ & band name (Eg)- TiO <sub>2</sub>	Peak position in $\text{cm}^{-1}$ & band name (Eg)- TiO <sub>2</sub>	Peak position in $\text{cm}^{-1}$ & band name (G)-RGO	Peak position in $\text{cm}^{-1}$ & band name (D)-RGO
ATO-(0)	641.93 $\text{cm}^{-1}$	518.51 $\text{cm}^{-1}$	398.94 $\text{cm}^{-1}$	198.38 $\text{cm}^{-1}$	148.24 $\text{cm}^{-1}$	-	-
ATO-(1)	613.96	518.51	449.08	238.88	146.31	-	-
ATO-(2)	613.96	nil	450.04	235.02	146.31	-	-
ATO-(3)	611.07	nil	446.19	239.84	148.24	-	-
ATO-(4)	613.0	nil	442.33	239.84	147.28	-	-
GATO-(0)	644.82	520.43	404.73	nil	154.03	1607.1 $\text{cm}^{-1}$	1357.4 $\text{cm}^{-1}$
GATO-(1)	641.93	520.43	404.73	nil	155.95	1598.5	1366.1
GATO-(2)	694.96*	618.79*	416.3	nil	nil	1588.0	nil
GATO-(3)	699.78*	609.14*	426.9*	262.02*	154.03	1602.31	1366.1
GATO-(4)	704.6*	610.113*	424.01*	nil	nil	1591.7	1355.05

### Resolved/ Magnified part of Raman spectrum for D and G peak:

Generally, the graphene sheet exhibits two most intense Raman bands around 1350  $\text{cm}^{-1}$  (D band), and 1580  $\text{cm}^{-1}$  (G band). The response of D band in Raman spectra is due to the presence of defects, dislocations, breakage of symmetry by edges and structural disorder in graphene sheets and is strongly influenced by excitation energy also. So the D peak is produced only in a small region of the crystal near a defect or an edge [S2-S5]. The G band arises from the first order scattering of the E2g phonon from the stretching of the  $\text{sp}^2$ -hybridized carbon-carbon bonds and is highly sensitive to strain effects and insensitive to defects, dislocations and structural disorder in  $\text{sp}^2$  system within graphene sheets. The D and G peak position of graphene incorporated Ag doped TiO<sub>2</sub> series are clearly observed except in case of GATO-(2) sample. The certain Raman bands of vibration in case of some samples are also absent; for instance sample ATO-(2) has four allowed modes of vibration while ATO-(1) has all six allowed modes. In case of ATO-(2) sample, the Eg Raman band assigned at 613.96  $\text{cm}^{-1}$  is very low in intensity in comparison to other samples, is an indication for dominating rutile phase of TiO<sub>2</sub> nanoparticles as the intensity of this band again increases for the sample ATO-(3), and ATO-(4) respectively. This is due to the reappearance of anatase phase for these samples as clearly observed in XRD pattern. The Eg, B1g, A1g mode and second-order scattering features (around 238.88  $\text{cm}^{-1}$  in ATO-(1) sample) are the major features in the Raman spectra of all the samples, while the other

like B<sub>2g</sub> (around 826 cm<sup>-1</sup>) modes are absent. Single layer graphene consists six normal modes named as A<sub>2u</sub>, B<sub>2g</sub>, E<sub>1u</sub>, and E<sub>2g</sub> (two modes are doubly degenerate modes) at the centre of Brillouin zone centre in reciprocal lattice plane. E<sub>2g</sub> is one degenerate in-plane optical mode, while B<sub>2g</sub> is

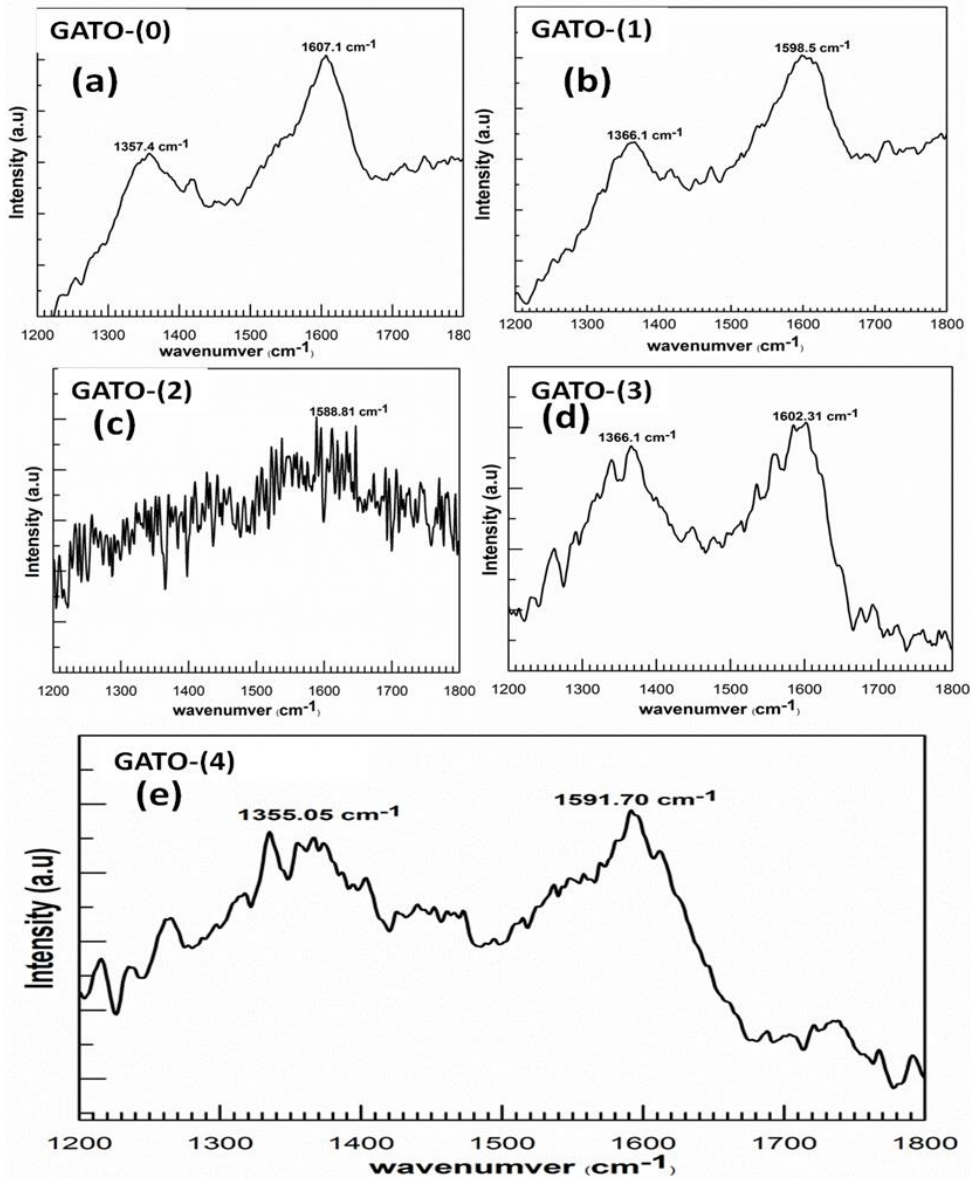


**Figure S-12.** Magnified part of Raman spectrum for graphene incorporated Ag doped TiO<sub>2</sub> samples; (a) GATO-(0), (b) GATO-(1), (c) GATO-(2), (d) GATO-(3), and (e) GATO-(4).

another degenerate out-of-plane optical mode. The E<sub>2g</sub> phonons are Raman active, whereas the B<sub>2g</sub> phonon is neither Raman nor infrared active. The peaks positioned at higher wave number sides are attributed to G band, while positioned at lower wave number sides are attributed to D band of RGO as listed in Table 3. In addition to this, the peak at 694.96 cm<sup>-1</sup> is seen as an

additional unresolved band (labelled as \* in Table 3) for multiphase GATO-(2) sample. All such unresolved bands are labelled as (\*) in case of GATO-(2), GATO-(3), and GATO-(4) samples respectively. Although we consider these bands exist because of huge anomalous shift in their main vibrating band (as listed in each column of the Table 3) due to shape-size dependent modifications, the formation of an additional AgCl phase and the formation of amorphous reduced graphene oxide also as evident by XRD, EDX/colour mapping and HRTEM [S2-S3]. The red shift in G and D band peak position have been also observed for graphene decorated Ag doped TiO<sub>2</sub> with respect to graphene decorated pure anatase TiO<sub>2</sub> sample (GATO-(0)). On the basis of this the charge transfer mechanism between RGO and the hybridized components can be verified by the Raman spectra also as discussed in UV-visible spectroscopy study. The G-band of RGO shifts towards lower wave number when RGO is hybridized with an electron donor component, while it shifts to higher wave number when an electron acceptor component is hybridized [S4]. In fact an increase of the G-peak intensity at high doping levels (as observed in GATO-(1) sample) is due to the change in electronic states done by doping. The doping can effectively exclude (so called an empty state) some regions of electronic wave vector (k), for two possible forbidden transitions (i) either a transition from an empty state (ii) or a transition to a filled state due to Pauli blocking [S5]. In recent studies it has also shown that Ag and TiO<sub>2</sub> generally behave like as electron donor while RGO and AgCl (in exceptional case) may act as an electron acceptor depending on its electronic structure and involved synthesizing mechanism. Therefore by considering all these facts the observed band gap for GATO-(3), and GATO-(4) samples are 0.1 eV and 0.2 eV higher than the GATO-(2) sample respectively, which is in good agreement with previously published results [S1, S6-S7].

## References

- [S1]. Virendra Singh et. al. Progress in Materials Science. 2011, **56**, 1178.
- [S2]. Hui Zhang et. al. Environ. Sci. Technol. 2011, **45**, 5731.
- [S3]. Varghese Swamy et. al. Appl. Phys. Lett. 2006, **89**, 163118.
- [S4]. A. H. Castro Neto et. al. Reviews of modern physics. 2009, **81**, 109.
- [S5]. Andrea C. Ferrari et. al. Nature Nanotechnology. 2013, **8**, 235.
- [S6]. Mohan Chandra Mathpal et. al. Chemical Physics Letters. 2013, **555**, 182.
- [S7]. Shu Jun Wang et. al. Carbon. 2010, **48**, 1815.